Unexpected Selectivities in C−H Activations of Toluene and *p*-Xylene at Cationic Platinum(II) Diimine Complexes. New Mechanistic Insight into Product-Determining Factors

Lars Johansson,[1a,b] Olav B. Ryan,[1c] Christian Rømming,[1a] and Mats Tilset*,[1a,d]

Contribution from the Department of Chemistry, University of Oslo, P.O. Box 1033 Blindern, N-0315 Oslo, Norway, and Department of Hydrocarbon Process Chemistry, SINTEF Applied Chemistry, P.O. Box 124 Blindern, N-0314 Oslo, Norway

Received January 31, 2001

Abstract: The C−H activation of toluene and *p*-xylene at cationic Pt^{II} diimine complexes (N−N)Pt(CH_3)(H_2O)$^+BF_4^-$ (N−N = Ar−N=CMe−CMe=N−Ar; **1**(BF_4^-), N^f−N^f, Ar = 3,5-$(CF_3)_2C_6H_3$); **2**(BF_4^-), N′−N′, Ar = 2,6-$(CH_3)_2C_6H_3$) has been investigated. The reactions were performed at ambient temperature in 2,2,2-trifluoroethanol (TFE), and after complete conversion of the starting material to mixtures of Pt-aryl/Pt-benzyl complexes and methane, acetonitrile was added to trap the products as more stable acetonitrile adducts. In the reactions with toluene, the relative amounts of products resulting from aromatic C−H activation were found to decrease in the order (N−N)Pt(*m*-tolyl)(NCMe)$^+$ > (N−N)Pt(*p*-tolyl)(NCMe)$^+$ > (N−N)Pt(*o*-tolyl)(NCMe)$^+$ for both **1** and **2**. Unlike the reaction at **1**, significant amounts of the benzylic activation product (N′−N′)Pt(benzyl)(NCMe)$^+$ were concurrently formed in the C−H activation of toluene at **2**. The C−H activation of *p*-xylene revealed an even more remarkable difference between **1** and **2**. Here, the product ratios of (N−N)Pt(xylyl)(NCMe)$^+$ and (N−N)Pt(*p*-methylbenzyl)(NCMe)$^+$ were found to be 90:10 and 7:93 for reactions at **1** and **2**, respectively. The elimination of toluene from (N^f−N^f)Pt($Tol)_2$ species (**3a**−**c**; **a**, Tol = *o*-tolyl; **b**, Tol = *m*-tolyl; **c**, Tol = *p*-tolyl) after protonolysis with 1 equiv of HBF_4 was investigated. Most notably, protonation in neat TFE followed by addition of acetonitrile gave a 77:23 mixture of (N^f−N^f)Pt(*m*-tolyl)(NCMe)$^+$ (**4b**) and (N^f−N^f)Pt(*p*-tolyl)(NCMe)$^+$ (**4c**) from all three isomeric bis(tolyl) complexes **3a**−**c**. The presence of acetonitrile during the protonation reactions resulted in considerably less isomerization. This behavior is explained by an associative mechanism for the product-determining displacement of toluene by the solvent. For the C−H activation reactions, our findings suggest the existence of a dynamic equilibrium between the isomeric intermediates (N−N)Pt(aryl)(CH_4)$^+$ (aryl = tolyl/benzyl from **1**; xylyl/*p*-methylbenzyl from **2**). The observed selectivities might then be explained by steric and electronic effects in the pentacoordinate transition-state structures for the solvent-induced associative elimination of methane from these intermediates.

Introduction

The development of practical methods for mild and selective functionalization of unactivated C−H bonds in hydrocarbons remains a challenge to chemists, motivated by important potential applications in natural gas conversion as well as organic synthesis.[2] During the past decades, important contributions toward this goal have been demonstrated in the field of homogeneous organometallic chemistry. In particular, approaches based on the remarkable "Shilov system",[3] discovered almost 30 years ago, hold promise for future advances.[4] In the Shilov system, simple alkanes are catalytically converted to mixtures of alcohols and chloroalkanes in aqueous solutions of Pt^{II} and Pt^{IV} salts. The mechanism for this reaction has been the subject of extensive investigations, and the three primary steps shown in Scheme 1 have been proposed: (i) C−H activation at Pt^{II}, (ii) oxidation by Pt^{IV}, and (iii) nucleophilic attack to yield the products and regeneration of the catalyst.[5] It has been considered of particular interest to elucidate the nature of the activation process (i) in the cycle, since this step is believed to dictate both the rate and the unusual chemo- and regioselectivity in the reaction. Insight into the mechanism has been gained through studies on stoichiometric model reactions between cationic Pt^{II} complexes and hydrocarbons,[6] as well as the reverse reaction—elimination of alkanes from Pt^{IV} hydridoalkyl species.[7] The C−H activation mechanism at Pt^{II} has also been addressed in theoretical investigations.[8]

Scheme 1

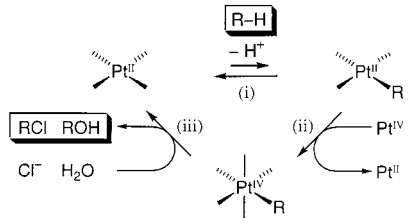

(1) (a) University of Oslo. (b) Current address: Department of Organic Chemistry, Arrhenius Laboratory, Stockholm University, S-106 91 Sweden. (c) SINTEF. (d) E-mail: mats.tilset@kjemi.uio.no.

(2) (a) Crabtree, R. H. *Chem. Rev.* **1995**, *95*, 987. (b) Arndtsen, B. A.; Bergman, R. G.; Mobley, T. A.; Peterson, T. H. *Acc. Chem. Res.* **1995**, *28*, 154. (c) Shilov, A. E.; Shulpin, G. B. *Chem. Rev.* **1997**, *97*, 2879. (d) Stahl, S. S.; Labinger, J. A.; Bercaw, J. E. *Angew. Chem., Int. Ed.* **1998**, *37*, 2180. (e) Shilov, A. E.; Shul'pin, G. B. *Activation and Catalytic Reactions of Saturated Hydrocarbons in the Presence of Metal Complexes*; Kluwer: Boston, 2000.

(3) Goldshlegger, N. F.; Eskova, V. V.; Shilov, A. E.; Shteinman, A. A. *Zh. Fiz. Khim.* **1972**, *46*, 1353. See also ref 2e.

(4) (a) Sen, A. *Acc. Chem. Res.* **1998**, *31*, 550. (b) Periana, R. A.; Taube, J. D.; Gamble, S.; Taube, H.; Satoh, T.; Fujii, H. *Science* **1998**, *280*, 560.

10.1021/ja010277e CCC: $20.00
Published on Web 06/19/2001

Scheme 2

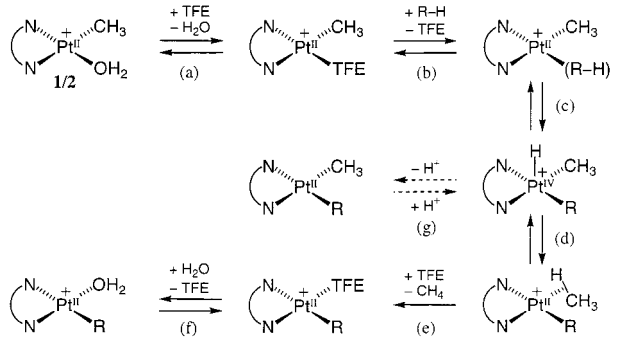

We have recently reported the development of Pt^{II} diimine (diimine = N—N = Ar—N=CMe—CMe=N—Ar)-based systems that activate methane and benzene C—H bonds.[9,10] The aqua complex $(N^f—N^f)Pt(CH_3)(H_2O)^+BF_4^-$ (**1**(BF_4^-); Ar = 3,5-$(CF_3)_2C_6H_3$) was demonstrated to react with benzene and methane in the hydroxylic solvent 2,2,2-trifluoroethanol (TFE) under unusually mild conditions.[9a,b] The benzene C—H activation at the closely related complex (N′—N′)$Pt(CH_3)(H_2O)^+BF_4^-$ (**2**(BF_4^-); Ar = 2,6-$(CH_3)_2C_6H_3$) was investigated in detail.[9c] Kinetic studies, labeling experiments, and low-temperature NMR characterization of possible intermediates in combination with theoretical calculations[9b] have led to the proposal of a common mechanism for these reactions (Scheme 2). A preequilibrium between the aqua and solvento complexes (N—N)$Pt(CH_3)(H_2O)^+$ and (N—N)$Pt(CH_3)(TFE)^+$ (a) is followed by rate-determining coordination of the hydrocarbon R—H (b) to give a hydrocarbon adduct (N—N)$Pt(CH_3)(R—H)^+$. These exchange processes appear to proceed via associative mechanisms.[9c,d] The hydrocarbon adduct rapidly interconverts via a transient Pt^{IV} hydride intermediate (N—N)$Pt(CH_3)(R)(H)^+$ (c) with an η^2-C,H-methane adduct (N—N)$Pt(R)(CH_4)^+$ (d). The reaction is completed by irreversible methane loss from (N—N)$Pt(R)(CH_4)^+$ via exchange reactions with solvent and water (e—f) to afford the corresponding Pt^{II} cations (N—N)$Pt(R)(H_2O)^+$. In addition, we have observed that reversible deprotonation of the putative (N—N)$Pt^{IV}(CH_3)(R)(H)^+$ intermediate takes place in the presence of considerable amounts of water (g).[11] These reactions are believed to be reasonable models for the activation in the Shilov system.

A key feature in the Shilov-type systems is the unprecedented regio- and chemoselectivity. Thus, contrary to the selectivity in radical and superacid reactions, the reactivity order 1° C—H > 2° > 3° is generally observed for alkanes.[12] Furthermore, from studies on the oxidation of ethane and ethanol in the aqueous Pt^{II}/Pt^{IV} system, the relative rate of C—H bond activation was found to decrease in the order $H—CH_2CH_3$ > $H—CH_2CH_2OH$ > $H—CH(OH)CH_3$,[5c,13] contrary to the trend expected from the homolytic bond strengths. The C—H activation step has been proposed to govern the unusual selectivity in the Shilov system. However, since the detailed mechanism for this process has been unclear, definite explanations for the observed selectivities have not been given.

A specific regioselectivity issue in C—H activation processes is related to reactions with alkylarenes in which competition between different aromatic and benzylic C—H bonds is possible. Results from studies on such reactions have been reported for some homogeneous organometallic systems. Jones and Feher observed a statistical 2:1 ratio of Cp*(PMe_3)Rh(*m*-Tol)(H) and Cp*(PMe_3)Rh(*p*-Tol)(H) as the only products from photolysis of Cp*(PMe_3)RhH_2 in toluene under conditions of thermodynamic product control.[10,14] When the reaction was performed at low temperature, small amounts of Cp*(PMe_3)Rh(*o*-Tol)(H) and traces of Cp*(PMe_3)Rh(Bz)(H) were also detected. The kinetic meta/para selectivity in this system was explained in terms of arene π-precoordination and steric effects. Whitesides and co-workers reported that thermal decomposition of *trans*-$(PMe_3)_2Pt(Np)(OTf)$ in toluene at 133 °C followed by treatment with chloride yielded a statistical 2:1 ratio of *trans*-$(PMe_3)_2Pt$-(*m*-Tol)(Cl) and *trans*-$(PMe_3)_2Pt(p$-Tol)(Cl).[15] A kinetic preference for aromatic C—H activation was found when (P—P)Pt(Np)(H) (P—P = bis(dicyclohexylphosphino)ethane) was heated at 69 °C in mesitylene.[16] Prolonged heating resulted in a slight excess of the benzylic activation product (P—P)Pt(3,5-Me_2Bz)(H) relative to the aromatic product (P—P)Pt(Mes)(H) (54:46), which was proposed to reflect the thermodynamic product distribution. The photolysis of Tp′Rh(CN—Np)(η-PhN=C=N—Np) in toluene at 25 °C was reported by Jones and Hessell to produce a mixture of Tp′Rh(R)(H)(CN—Np) species with R = *m*-tolyl, *p*-tolyl, and benzyl in a 2:4:3 ratio.[17] Heating of this mixture at 100 °C for 12 h resulted in complete conversion to a statistical 2:1 ratio of the *m*-tolyl and *p*-tolyl

(5) (a) Kushch, L. A.; Lavrushko, V. V.; Misharin, Y. S.; Moravsky, A. P.; Shilov, A. E. *Nouv. J. Chim.* **1983**, *7*, 729. (b) Horvath, I. T.; Cook, R. A.; Millar, J. M.; Kiss, G. *Organometallics* **1993**, *12*, 8. (c) Hutson, A. C.; Lin, M.; Basickes, N.; Sen, A. *J. Organomet. Chem.* **1995**, *504*, 69. (d) Labinger, J. A.; Herring, A. M.; Lyon, D. K.; Luinstra, G. A.; Bercaw, J. E.; Horvath, I. T.; Eller, K. *Organometallics* **1993**, *12*, 895. (e) Luinstra, G. A.; Labinger, J. A.; Bercaw, J. E. *J. Am. Chem. Soc.* **1993**, *115*, 3004. (f) Luinstra, G. A.; Wang, L.; Stahl, S. S.; Labinger, J. A.; Bercaw, J. E. *Organometallics* **1994**, *13*, 755. (g) Luinstra, G. A.; Wang, L.; Stahl, S. S.; Labinger, J. A.; Bercaw, J. E. *J. Organomet. Chem.* **1995**, *504*, 75.

(6) (a) Holtcamp, M. W.; Labinger, J. A.; Bercaw, J. E. *J. Am. Chem. Soc.* **1997**, *119*, 848. (b) Holtcamp, M. W.; Henling, L. M.; Day, M. W.; Labinger, J. A.; Bercaw, J. E. *Inorg. Chim. Acta* **1998**, *270*, 467. (c) Wick, D. D.; Goldberg, K. I. *J. Am. Chem. Soc.* **1997**, *119*, 10235.

(7) (a) Stahl, S. S.; Labinger, J. A.; Bercaw, J. E. *J. Am. Chem. Soc.* **1995**, *117*, 9371. (b) Stahl, S. S.; Labinger, J. A.; Bercaw, J. E. *J. Am. Chem. Soc.* **1996**, *118*, 5961. (c) Fekl, U.; Zahl, A.; van Eldik, R. *Organometallics* **1999**, *18*, 4156. (d) Hill, G. S.; Rendina, L. M.; Puddephatt, R. J. *Organometallics* **1995**, *14*, 4966. (e) Jenkins, H. A.; Yap, G. P. A.; Puddephatt, R. J. *Organometallics* **1997**, *16*, 1946.

(8) (a) Siegbahn, P. E. M.; Crabtree, R. H. *J. Am. Chem. Soc.* **1996**, *118*, 4442. (b) Hill, G. S.; Puddephatt, R. J. *Organometallics* **1998**, *17*, 1478. (c) Heiberg, H.; Swang, O.; Ryan, O. B.; Gropen, O. *J. Phys. Chem. A* **1999**, *103*, 10004. (d) Mylvaganam, K.; Bacskay, G. B.; Hush, N. S. *J. Am. Chem. Soc.* **1999**, *121*, 4633. (e) Mylvaganam, K.; Bacskay, G. B.; Hush, N. S. *J. Am. Chem. Soc.* **2000**, *122*, 2041. (f) Bartlett, K. L.; Goldberg, K. I.; Borden, W. T. *J. Am. Chem. Soc.* **2000**, *122*, 1456.

(9) (a) Johansson, L.; Ryan, O. B.; Tilset, M. *J. Am. Chem. Soc.* **1999**, *121*, 1974. (b) Heiberg, H.; Johansson, L.; Gropen, O.; Ryan, O. B.; Swang O.; Tilset, M. *J. Am. Chem. Soc.* **2000**, *122*, 10831. (c) Johansson, L.; Tilset, M.; Labinger, J. A.; Bercaw, J. E. *J. Am. Chem. Soc.* **2000**, *122*, 10846. (d) Johansson, L.; Tilset, M. *J. Am. Chem. Soc.* **2001**, *123*, 739.

(10) Abbreviations: Cp* = η^5-C_5Me_5; Tp′ = hydridotris(3,5-dimethylpyrazol)borate; Np = neopentyl; Tol = tolyl; Bz = benzyl; Xyl = xylyl; Mes = mesityl; OTf^- = triflate; $N^f—N^f$ = ArN=CMeCMe=NAr, Ar = 3,5-$(CF_3)_2C_6H_3$; N′—N′ = ArN=CMeCMe=NAr, Ar = 2,6-$(CH_3)_2C_6H_3$; TFE = trifluoroethanol.

(11) In a reaction between $(N^f—N^f)Pt^{II}(CH_3)(H_2O)^+$ (**1**) and C_6H_6 in a 4.0 M solution of D_2O in TFE-d_3, the formation of $(N^f—N^f)Pt^{II}(C_6H_5)$-$(H_2O)^+$ and CH_4, CH_3D, CH_2D_2, and traces of CHD_3 was observed by ^1H NMR spectroscopy (the analogous experiment in pure TFE-d_3 gives only CH_4). This experiment demonstrates that reversible deprotonation of the putative $(N^f—N^f)Pt^{IV}(CH_3)(R)(H)^+$ intermediate is readily induced by addition of water to the reaction medium, presumably due to the higher basicity of water compared to TFE. Importantly, this finding strengthens the relevance of the Pt^{II} diimine C—H activation reactions with respect to the Shilov system. Tilset, M.; Johansson L. Unpublished results.

(12) (a) Hodges, R. J.; Webster, D. E.; Wells, P. B. *J. Chem. Soc., Chem. Commun.* **1971**, 462. (b) Goldshlegger, N. F.; Lavrushko, V. V.; Khrush, A. P.; Shteinman, A. A. *Izv. Akad. Nauk., Ser. Khim.* **1976**, *10*, 2174.

(13) Sen, A.; Benvenuto, M. A.; Lin, M.; Hutson, A. C.; Basickes, N. *J. Am. Chem. Soc.* **1994**, *116*, 998.

(14) Jones, W. D.; Feher, F. J. *J. Am. Chem. Soc.* **1984**, *106*, 1650.

(15) Brainard, R. L.; Nutt, R.; Lee, R.; Whitesides, G. M. *Organometallics* **1988**, *7*, 2379.

(16) Hackett, M.; Whitesides, G. M. *J. Am. Chem. Soc.* **1988**, *110*, 1449.

(17) Jones, W. D.; Hessell, E. T. *J. Am. Chem. Soc.* **1993**, *115*, 554.

Scheme 3

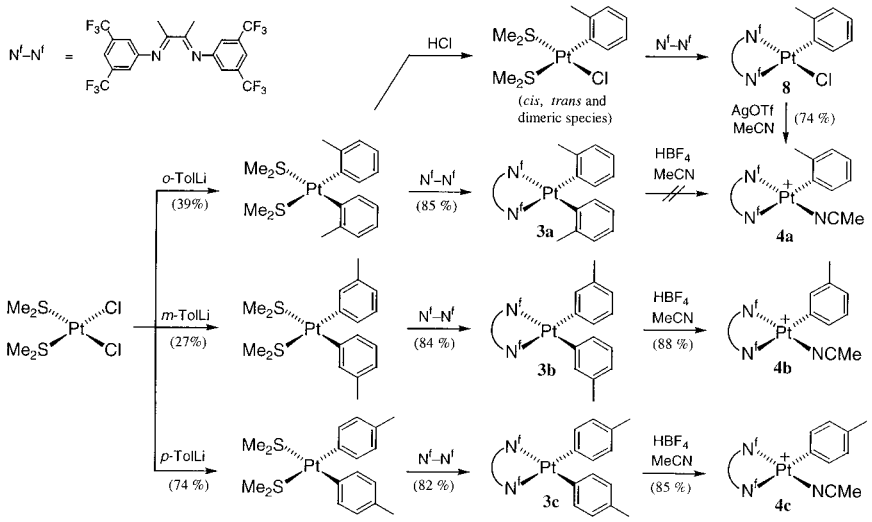

complexes. The authors remarked that this system exhibits an unusually large kinetic preference for benzylic activation. Bergman and Burger reported that reaction between Cp*(PMe_3)Ir(CH_3)(OTf) and toluene resulted in a 62:38 ratio of Cp*(PMe_3)Ir(*m*-Tol)(OTf) and Cp*(PMe_3)Ir(*p*-Tol)(OTf) as the only products, i.e., with a somewhat less than statistical amount of the meta isomer.[18] The absence of *o*-tolyl product was explained by steric effects. C−H activation of toluene has also been studied in reactions with the Pt^{IV} salt H_2PtCl_6 in acidic media at 50−90 °C.[19] The products were trapped as the anionic species *trans*-$PtCl_4(NH_3)(Tol)^-$, and at short reaction times the *p*-tolyl isomer was obtained as the dominant product. However, prolonged heating gave the statistical 2:1 ratio of the *m*-tolyl and *p*-tolyl complexes as the only observed products. Legzdins and co-workers[20] recently reported that thermal toluene C−H activation at Cp*W(NO)(CH_2CMe_3)$_2$ produced Cp*W(NO)(CH_2CMe_3)(Tol) in a 1:47:33 *o*:*m*:*p* ratio. The immediate product of benzylic C−H activation, Cp*W(NO)(CH_2CMe_3)(CH_2-Ph), was observed as an intermediate that reacted further to give other species that were also results of benzylic activation. Significantly, whereas prolonged heating of the *o*-tolyl or *m*-tolyl products separately resulted in isomerization to the 1:47:33 mixture of tolyl isomers, there was no interconversion of products of aromatic C−H activation into those of benzylic activation (or vice versa).

In this paper, regioselectivity issues in the Pt^{II} diimine system are addressed through investigations of the C−H activation of toluene (in which four different types of C−H bonds are available) and *p*-xylene (in which two different C−H bonds are available) at (N^f—N^f)Pt(CH_3)(H_2O)$^+$ (**1**) and (N′—N′)Pt(CH_3)(H_2O)$^+$ (**2**). The regioselectivities of these reactions depend strongly on the identity of the substrate and the metal complex and on the solvent composition. The results provide important mechanistic insight that helps us to understand the nature of the product-determining steps of these reactions.

Results

Synthesis and Characterization of Diimine Platinum(II) Tolyl Complexes. To facilitate product identification in the C−H activation reactions with toluene and *p*-xylene, preparation of (N^f—N^f)Pt(Tol)$_2$ (**3a**−**c**) and (N^f—N^f)Pt(Tol)(NCMe)$^+$ (**4a**−**c**) complexes (Tol = *o*-tolyl, **a**; *m*-tolyl, **b**; *p*-tolyl, **c**) was accomplished by the reactions outlined in Scheme 3. Since these species are new, their preparation and characterization will be described in some detail. Starting from Pt(SMe_2)$_2$$Cl_2$,[21] the *cis*-Pt($SMe_2$)$_2(Tol)_2$ species were synthesized by treatment with the appropriate tolyllithium reagent by methods similar to those described in the literature.[22a] Subsequent reaction with the diimine ligand N^f—N^f gave the corresponding (N^f—N^f)Pt(Tol)$_2$ complexes **3a**−**c** in excellent yields. For the *m*- and *p*-tolyl compounds **3b** and **3c**, protonation with 1 equiv of HBF_4·Et_2O in acetonitrile led to the formation of the BF_4^- salts of the corresponding species (N^f—N^f)Pt(*m*-Tol)(NCMe)$^+$ (**4b**) and (N^f—N^f)Pt(*p*-Tol)(NCMe)$^+$ (**4c**). In the latter reaction, small amounts of **4b** were observed as a byproduct (ca. 4% by ^{19}F NMR spectroscopy). Analytically and spectroscopically pure **4c**(BF_4^-) was obtained by recrystallization. Attempted preparation of (N^f—N^f)Pt(*o*-Tol)(NCMe)$^+$ (**4a**) by protonation of **3a** with HBF_4·Et_2O in acetonitrile led, however, to extensive positional isomerization and formation of a mixture of **4a**, **4b**, and **4c** in ca. 1:7:2 ratio. Consequently, an alternative synthetic route was worked out for the production of **4a**. Treatment of a dichloromethane solution of *cis*-Pt(*o*-Tol)$_2$(SMe_2)$_2$ with 1 equiv of HCl in ether gave a product mixture that exhibited a very complex product ^{1}H NMR spectrum, presumably due to the formation of a mixture of *cis*- and *trans*-Pt(*o*-Tol)(Cl)(SMe_2)$_2$ and the dimeric complexes *cis*- and *trans*-Pt$_2$(*o*-Tol)$_2$(Cl)$_2$(μ-SMe_2)$_2$. Further reaction of this mixture with the diimine ligand N^f—N^f produced (N^f—N^f)Pt(*o*-Tol)(Cl) (**8**). However, *trans*-Pt(*o*-Tol)(Cl)(SMe_2)$_2$ was found to be unreactive toward the ligand, even at elevated temperatures. Hence, a mixture of this species, free N^f—N^f ligand, and **8** was obtained after completion of the reaction. Separation of **8** from the unreacted material was accomplished by column chromatography on silica. Finally, treatment of **8** with AgOTf in THF/acetonitrile yielded (N^f—N^f)Pt(*o*-Tol)(NCMe)$^+$OTf$^-$ (**4a**(OTf$^-$)).

All new compounds were characterized by ^{1}H and ^{19}F NMR spectroscopy (key data are given in Table 1). The ^{1}H and ^{19}F

(18) Burger, P.; Bergman, R. G. *J. Am. Chem. Soc.* **1993**, *115*, 10462.
(19) (a) Shulpin, G. B.; Kitaygorodskiy, A. N. *J. Organomet. Chem.* **1981**, *212*, 275. (b) Shulpin, G. B.; Nizova, G. V.; Nikitaev, A. T. *J. Organomet. Chem.* **1984**, *276*, 115.
(20) Adams, C. S.; Legzdins, P.; Tran, E. *J. Am. Chem. Soc.* **2001**, *123*, 612.
(21) Hill, G. S.; Irwin, M. J.; Levy, C. J.; Redina, L. M.; Puddephatt, R. J. *Inorg. Synth.* **1998**, *32*, 149.
(22) (a) Rashidi, M.; Hashemi, M.; Khorasani-Motlagh, M.; Puddephatt, R. J. *Organometallics* **2000**, *19*, 2751. (b) Puddephatt, R. J.; Thomson, M. A. *J. Organomet. Chem.* **1982**, *238*, 231.

Table 1. Key ^{1}H and ^{19}F NMR Data for New Isolated Complexes

compound	^{1}H NMR, δ[a] Tol-*Me* ($^4J(^{195}$Pt−H))	diimine-*Me* ($^4J(^{195}$Pt−H))	aryl-H_o (relative intensity)	Pt-NC*Me* ($^4J(^{195}$Pt−H))	^{19}F NMR, δ aryl-CF_3 (relative intensity)
syn-(N^f—N^f)Pt(*o*-Tol)$_2$ (*syn*-**3a**)	2.31 (6.7)	1.71	7.17 (1)	−	−62.98 (1)
			7.37 (1)		−62.85 (1)
anti-(N^f—N^f)Pt(*o*-Tol)$_2$ (*anti*-**3a**)	2.13 (6.4)	1.71	7.28	−	−63.35
(N^f—N^f)Pt(*m*-Tol)$_2$ (**3b**)	1.89	1.81	7.25	−	−63.10
(N^f—N^f)Pt(*p*-Tol)$_2$ (**3c**)	2.04	1.79	7.24	−	−63.28
(N^f—N^f)Pt(*o*-Tol)(NCMe)$^+$ (**4a**)	2.37	2.23 (9.1)	7.44 (1)	2.08 (14.0)	−63.58 (1)
		2.37	7.47 (1)		−63.24 (1)
			8.03 (2)		−62.93 (2)
(N^f—N^f)Pt(*m*-Tol)(NCMe)$^+$ (**4b**)	1.96	2.25 (9.3)	7.39 (1)	2.09 (13.5)	−63.22 (1)
		2.36	7.96 (1)		−62.95 (1)
(N^f—N^f)Pt(*p*-Tol)(NCMe)$^+$ (**4c**)	2.09	2.25 (9.8)	7.37 (1)	2.09 (13.8)	−63.45 (1)
		2.36	7.96 (1)		−62.94 (1)

[a] Dichloromethane-d_2.

Table 2. Crystal Data and Structure Refinement for *syn*-**3b**

empirical formula	$C_{34}H_{26}F_{12}N_2Pt\cdot CH_2Cl_2$	*F*(000)	1880
formula weight	968.57	crystal size	0.18 × 0.8 × 0.8 mm
temperature	150(2) K	θ-range for data	10.24 to 30.50°
wavelength	0.71073 Å	reflections collected	45877
crystal system	orthorhombic	independent reflections	5386 [*R*(int) = 0.056]
space group	*Pnma*	refinement method	full-matrix least- squares on F^2
unit cell dimensions	a = 14.659(2) Å	data/parameters	5386/241
	b = 25.664(3) Å	goodness-of-fit on F^2	1.219
	c = 9.624(2) Å	final *R* indices [$I > 2\sigma(I)$]	$R1$ = 0.055, w$R2$ = 0.121
volume, *Z*	3620.9(9) Å^3, 4	*R* indices (all data)	$R1$ = 0.068, w$R2$ = 0.129
density (calculated)	1.657 Mg/m^3	$\Delta\rho$(max)	2.53 e·Å^{-3}
absorption coefficient	4.113 mm^{-1}	$\Delta\rho$(min)	−2.73e·Å^{-3}

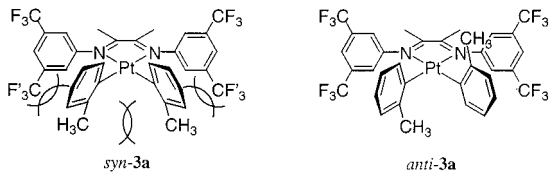

Figure 1. Rotamers *syn*-**3a** and *anti*-**3**a. The steric interactions indicated for *syn*-**3a** are proposed to account for the restricted rotation of the diimine aryl moieties and the observation of separate signals for the CF_3 and CF_3' groups in the ^{19}F NMR spectrum.

NMR spectra of **3b** and **3c** clearly reflect the molecular symmetry of these species. Thus, the aryl CF_3 groups gave rise to one signal in the ^{19}F NMR spectra for each complex. The two compounds exhibit quite similar ^{1}H NMR spectra, with the exception of the signal pattern for the tolyl group resonances.

For the closely related species **3a**, the NMR analysis revealed a more complex situation. Thus, in the ^{1}H NMR spectrum, two sets of signals were seen in ca. 54:46 ratio, each corresponding to the (N^f—N^f)Pt(*o*-Tol)$_2$ formulation. We believe that the two species are rotamers, differing in having the two tolyl-*Me* groups oriented mutually syn or anti with respect to the coordination plane of Pt (Figure 1). Apparently, the interconversion of the two rotamers must be slow on the NMR time scale. Furthermore, a significant difference between the two species was observed by NMR spectroscopy. Whereas the minor isomer exhibited only one signal for the diimine aryl-*H*(2,6) and as well as for the CF_3 groups in the ^{1}H and ^{19}F NMR spectra, the corresponding groups in the major isomer gave rise to two resonances in a 1:1 ratio in each spectrum. This observation suggests that for the major isomer, rotation around the diimine N—C$_{Aryl}$ axes must also be restricted. We tentatively propose the identities of the major and minor rotamer to be *syn*-**3a** and *anti*-**3a**, respectively. Steric interactions between the two tolyl-*Me* groups in *syn*-**3a** is suggested to restrict the rotational freedom of the tolyl rings (as indicated in Figure 1), thereby blocking rotation of the diimine aryl rings. Efficient rotation of the aromatic rings may require concerted movements of all four rings. Restricted rotation causes the diimine aryl-H(2,6) and CF_3 groups "above" and "below" the coordination plane in *syn*-**3a** to be chemically nonequivalent, which in turn leads to separate chemical shifts in the NMR spectra.

The ^{1}H and ^{19}F NMR spectra of the cationic acetonitrile species (N^f—N^f)Pt(*m*-Tol)(NCMe)$^+$ (**4b**) and (N^f—N^f)Pt(*p*-Tol)-(NCMe)$^+$ (**4c**) are in accordance with complexes of lower symmetry compared to the precursors **3b** and **3c**. Separate signals for the CF_3 substituents on each of the two diimine aryl rings were seen by ^{19}F NMR spectroscopy. In the ^{1}H NMR spectra, ^{195}Pt satellites were observed for one of the methyls on the backbone of the diimine ligand ($^4J(^{195}$Pt—H) ca. 9 Hz). Based on relative trans effect arguments, these methyl groups are presumably the ones transoid to the acetonitrile ligand.[23]

Once again, somewhat different NMR features were found for the *o*-tolyl analogue (**4a**). In the ^{19}F NMR spectrum, three signals for the aryl CF_3 groups appeared in a 2:1:1 ratio. A similar pattern of signals was observed for the diimine aryl-H(2,6) signals in the ^{1}H NMR spectrum. Apparently, steric interactions between the *o*-tolyl-*Me* group and the neighboring diimine aryl moiety prevent free rotation of these two rings. In analogy to the discussion above, this gives rise to chemically nonequivalent substituents "above" and "below" the coordination plane on this diimine aryl ring. The second diimine aryl ring is sterically less encumbered and rotates freely.

Importantly, the differences in the ^{19}F NMR signal patterns for the cationic complexes **4a**−**c** were of particular value for

(23) Complete ^{1}H and ^{13}C NMR assignment of the closely related species (N—N)Pt(CH$_3$)(NCMe)$^+$BF$_4^-$ (N—N = Ar—N=CH—CH=N—Ar; Ar = 4-MeOC$_6$H$_4$) demonstrated that the trends in $J(^{195}$Pt—H) data might be rationalized by relative ligand trans effects. Johansson, L.; Ryan, O. B.; Rømming, C.; Tilset, M. *Organometallics* **1998**, *17*, 3957.

Table 3. Selected Bond Lengths (Å) and Angles (deg) for *syn*-**3b**

Pt(1)−C(11)	2.010(6)	Pt(1)−N(1)	2.086(4)
N(1)−C(1)	1.285(7)	N(1)−C(3)	1.437(7)
C(1)−C(1A)	1.501(11)	C(1)−C(2)	1.485(8)
N(1)−Pt(1)−C(11)	97.0(2)	N(1)−Pt(1)−C(11A)	171.6(2)
N(1)−Pt(1)−N(1A)	75.7(2)	C(11)−Pt(1)−C(11A)	90.0(3)
Pt(1)−N(1)−C(1)	117.4(4)	Pt(1)−N(1)−C(3)	121.2(4)
C(1)−N(1)−C(3)	121.4(5)	N(1)−C(1)−C(2)	125.8(5)
N(1)−C(1)−C(1A)	114.3(3)	C(2)−C(1)−C(1A)	119.9(4)

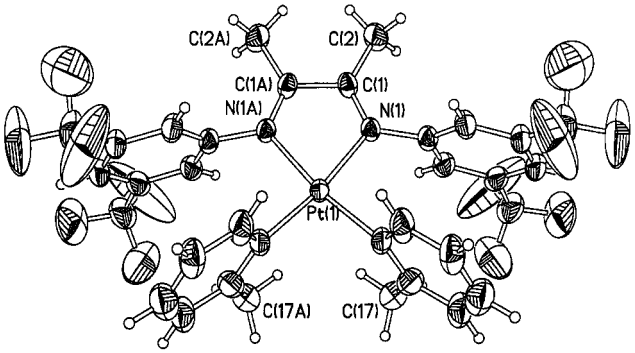

Figure 2. ORTEP plot of the structure of *syn*-**3a**.

the analysis of the product mixtures in the toluene activation reaction (vide infra).

X-ray Crystallographic Structure Determination of *syn*-3a. Crystals of quality suitable for X-ray diffraction analysis were obtained by slow evaporation of a dichloromethane solution of **3a**. Details about the structure determination are given in the Experimental Section. Table 2 lists experimental and crystallographic data, and selected bond distances and angles are given in Table 3. Figure 2 shows an ORTEP drawing of the X-ray crystal structure of **3a**, revealing that the complex has crystallized in the geometry where the tolyl-*Me* groups are oriented mutually syn with respect to the coordination plane of Pt. (No attempts have been made to establish whether **3a** crystallizes exclusively in the syn form, or whether crystals of the anti form might also be present in the isolated solid.) A crystallographic mirror plane is located perpendicular to the coordination plane, bisecting the chelate C−C bond and passing through the Pt atom, and gives rise to a molecular C_s symmetry. The diimine arene rings are twisted away from the tolyl-*Me* groups at an angle relative to the chelate ring plane of 86.1°. This geometry is probably assumed in order to minimize steric repulsions between the diimine arene moieties and the tolyl-*Me* and the chelate-*Me* groups. Interestingly, the orientation of the two tolyl rings is essentially perpendicular to the chelate ring (chelate ring/tolyl ring interplanar twist angle 90.4°). This orientation brings the two tolyl-*Me* groups into close proximity with each other. The steric repulsions caused by this interaction are presumably alleviated through a significant distortion of the square-planar geometry at the metal center: the Pt−C_{Tol} bonds are bent down relative to the chelate ring plane in Figure 2 by an angle of 7.8°.

C−H Activation of Toluene. The C−H activation of toluene was performed at ambient temperature in TFE-d_3. To probe possible diimine ligand effects on the selectivity, both **1** and the sterically more congested **2**[24] were studied under otherwise identical reaction conditions (Figure 3). The reaction between **1**(BF_4^-) and 30 equiv of toluene (ca. 0.4 M) in TFE-d_3 was monitored by ^{1}H and ^{19}F NMR spectroscopy at ambient

(24) In TFE solution, **2** is in equilibrium with a minor solvento complex (N′−N′)Pt(CH_3)(TFE)$^+BF_4^-$; K_{eq} = [(N′−N′)Pt(CH_3)(TFE)$^+$][H_2O]/[**2**]-[TFE] ≈ 1.2 ± 0.3 × 10^{-3} at 25 °C. See ref 9c.

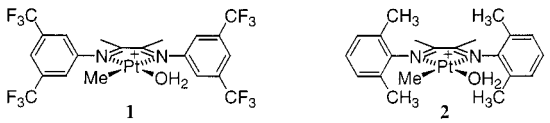

Figure 3. Cationic aqua species (N^f−N^f)Pt(CH_3)(H_2O)$^+$ (**1**) and (N′−N′)Pt(CH_3)(H_2O)$^+$ (**2**).

Scheme 4

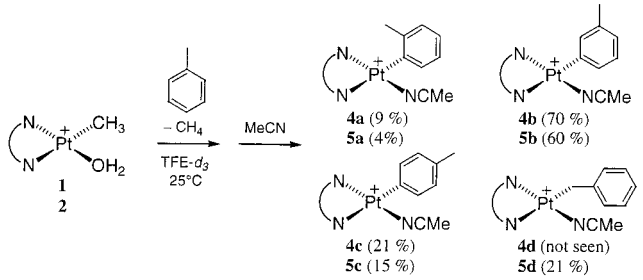

Scheme 5

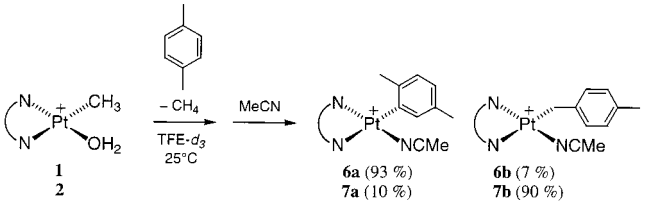

temperature. After complete reaction (ca. 3 h), acetonitrile was added to convert all species to the corresponding acetonitrile adducts. The resulting mixture of products was then analyzed in dichloromethane-d_2 by ^{1}H and ^{19}F NMR spectroscopy. As shown in Scheme 4, a mixture of **4a**, **4b**, and **4c** was found in a 9:70:21 ratio. No traces of the benzylic C−H activation product **4d** were observed in the reaction. The reaction of **2**(BF_4^-) with toluene was carried out in TFE-d_3 under identical conditions. As anticipated from the observed reaction rates with benzene,[9b,c] the activation of toluene at **2** was found to be somewhat slower than that of **1** (ca. 24 h for complete conversion). Identification of the acetonitrile adducts in the resulting product mixture was based solely on assignment of the signals in the ^{1}H NMR spectra in dichloromethane-d_2 (i.e., the complexes **5a**−**d** were not independently synthesized). However, the ^{1}H NMR spectroscopic features of the analogous species **4a**−**c** significantly aided the analysis and assignments of the products. As can be seen in Scheme 4, the product mixture consisted of **5a**, **5b**, **5c**, and **5d** in a 4:60:15:21 ratio. Complex **5d** was readily identified by its Pt−methylene signal at δ 2.68, accompanied by characteristic ^{195}Pt satellites ($^2J(^{195}\text{Pt}-\text{H})$ = 102 Hz). Thus, unlike the reaction at **1**, a substantial amount of benzylic C−H activation occurs at **2**. The ratio between the *o*-, *m*- and *p*-tolyl species **5a**, **5b**, and **5c** was found to be approximately the same as in the activation at **1**.

C−H Activation of *p*-Xylene. The complexes **1**(BF_4^-) and **2**(BF_4^-) were treated with *p*-xylene in experiments (Scheme 5) that were conducted in the same manner as the toluene activation reactions described above. In the reaction with **1**, the products were identified as **6a** (93%) and **6b** (7%) (key ^{1}H NMR data are given in Table 4), establishing that aromatic C−H activation is preferred over benzylic reaction. In sharp contrast to this, the reaction between **2** and *p*-xylene led to almost exclusive formation of the benzylic product **7b** (90%). A small amount of **7a** (10%) was also observed in the reaction.

Protonolysis of the (N^f−N^f)Pt(Tol)$_2$ Complexes 3a−c and (N′−N′)Pt(*p*-Tol)$_2$ (9c). As mentioned above, attempted syn-

Table 4. Key ^{1}H NMR Data for Products Formed in the C−H Activation of *p*-Xylene at **1** and **2**

	^{1}H NMR, δ^a			
Compound	PtCH_2 ($^2J(^{195}$Pt−H))	Xyl/Bz *Me*	diimine N=C(*Me*)	Pt−NC*Me* ($^4J(^{195}$Pt−H))
$(N^f{-}N^f)Pt(Xyl)(NCMe)^+$ (**6a**)	−	1.96 (Me_m) 2.34 (Me_o)	2.21 2.35	2.08 (13.8)
$(N^f{-}N^f)Pt(p\text{-MeBz})(NCMe)^+$ (**6b**)	2.78 (101.9)	na	na	1.81 (na)
$(N'{-}N')Pt(Xyl)(NCMe)^+$ (**7a**)	−	1.97 (Me_m) 2.46 (Me_o)	2.11 2.20	1.86 (13.7)
$(N'{-}N')Pt(p\text{-MeBz})(NCMe)^+$ (**7b**)	2.64 (101.4)	2.12	2.02 2.07	1.68 (13.9)

[a] Dichloromethane-d_2. na, not applicable.

Table 5. Product Mixtures Obtained after Protonation of Complexes **3a**−**c** with 1 Equiv of $HBF_4{\cdot}Et_2O$

		Products (%)		
Reactant	Solvent [a]	**4a**	**4b**	**4c**
3a	A	–	77	23
	B	–	65	35
	C	7	57	36
3b	A	–	77	23
	B	–	93	7
	C	–	100	–
3c	A	–	77	23
	B	–	22	78
	C	–	4	96

[a] (A) TFE; addition of MeCN after completed reaction. (B) 1.7 M MeCN in TFE. (C) MeCN.

thesis of **4a** by protonation of the corresponding bis(*o*-tolyl) complex **3a** in acetonitrile gave a mixture of **4a**, **4b**, and **4c**. Since this behavior was in striking contrast to that of the analogous complexes **3b** and **3c**, we wanted to better understand the factors that caused this outcome. Each of the three bis(tolyl) species **3a**−**c** were protonated with 1 equiv of $HBF_4{\cdot}Et_2O$ in neat acetonitrile, 1.7 M acetonitrile in TFE, and neat TFE. For the reactions that were performed in neat TFE, acetonitrile was added after completed reactions to trap the products as the corresponding acetonitrile adducts. As can be seen from the results (Table 5), the extent of isomerization was found to be highly dependent on the solvent system. *Most notably, a 77:23 mixture of **4b** and **4c** was obtained from all three bis(tolyl) complexes **3a**−**c** in the reactions that were done in neat TFE.* The presence of 1.7 M acetonitrile clearly inhibited the isomerization, and in neat acetonitrile the reactions of **3b** and **3c** proceeded to almost exclusively yield the corresponding cationic acetonitrile adducts **4b** and **4c**. The absence of the *o*-tolyl product **4a** in all reactions (except the 7% produced in the protonation of **3a** in acetonitrile) manifests that its formation is highly unfavorable when compared to the isomeric products.

An experiment was also performed where $(N'{-}N')Pt(p\text{-Tol})_2$ (**9c**; prepared from *cis*-$Pt(SMe_2)_2(p\text{-Tol})_2$ and the diimine ligand N′−N′) was protonated with 1 equiv of $HBF_4{\cdot}Et_2O$ in a 0.05 M solution of acetonitrile in TFE. As shown in Scheme 6, the product mixture consisted of **5a**, **5b**, **5c**, and **5d** in an 8:65:15:12 ratio. This product distribution is similar to that obtained in the toluene activation at **2**. Importantly, the formation of significant amounts of the benzylic isomer **5d** in this reaction implies that toluene is capable of rapidly rearranging between "aromatic" and "benzylic" C−H bond coordination modes prior to elimination.[25]

Scheme 6

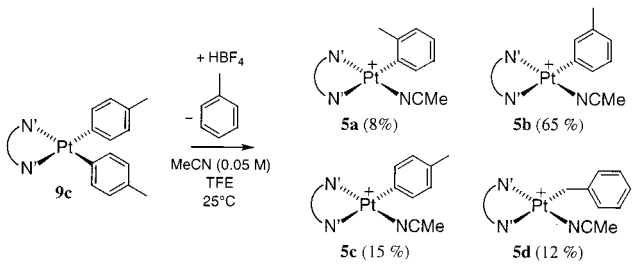

(25) In a TFE-d_3 solution of $(N'{-}N')Pt(C_6H_5)(NCMe)^+$ [9c] in the presence of 0.4 M toluene, no formation of the corresponding $(N'{-}N')Pt(Tol)(NCMe)^+$ complexes could be observed by ^{1}H NMR spectroscopy after 24 h at ambient temperature. This control experiment suggests that the observed isomerization in the protonation experiment is not due to re-coordination and activation of toluene at the produced $(N'{-}N')Pt(Tol)(NCMe)^+$ complexes.

Scheme 7

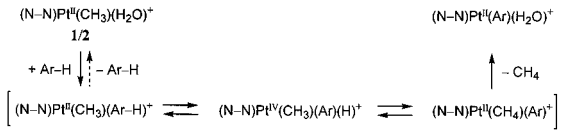

Discussion

We expect that the reactions of **1** and **2** with toluene and *p*-xylene proceed analogously to the general pathways established for benzene and methane in previous investigations (Scheme 2).[9b,c] Thus, rate-limiting exchange of the aromatic substrate for coordinated water at the starting complex gives the corresponding toluene or *p*-xylene adduct intermediate (Scheme 7).[26] Subsequent reversible cleavage of an arene C−H bond produces a Pt^{IV} hydride which undergoes methyl-H coupling to yield a methane adduct. Irreversible elimination of methane and coordination of water complete the reaction.

Substantial experimental evidence obtained from the mechanistic studies on the benzene and methane activation systems suggests that a TFE-assisted associative mechanism operates for the water/hydrocarbon exchange at platinum (i.e., the first and the last steps in Scheme 7). For the benzene C−H activation at **2**, this was corroborated by (1) a rate law first-order in [C_6H_6] as well as [**2**] and inverse first-order in [H_2O], and (2) rather negative activation entropy (−16 cal mol^{-1} K^{-1}) for the reaction.[9c] The methane activation at **1** was also found to be inhibited by addition of water, in accordance with reversible predissociation of water prior to methane coordination. The microscopic reverse of the methane activation−elimination of methane through protonolysis of (N^f−N^f)Pt(CH$_3$)$_2$ and (N′−N′)Pt(CH$_3$)$_2$ with DOTf in TFE-d_3—was also examined.[9d] In these experiments, the extent of methyl/methane H/D scrambling (effected by an equilibrium analogous to the one within the brackets in Scheme 7) was found to be *dependent* on the concentration of small amounts of added acetonitrile. Thus, at higher [MeCN], less H/D scrambling occurred. This finding strongly suggests that the mechanism for acetonitrile/methane exchange is also associative, given that the final methane loss is irreversible under the reaction conditions.

The results from the C−H activation and protonation reactions in the present study provide further evidence for associative pathways for the hydrocarbon/solvent exchange in these systems. Unequivocal evidence for meta preference is observed in the toluene C−H activation as well as the protonation reactions of the bis(tolyl) complexes **3a**−**c** and **9c** in TFE in the absence of acetonitrile. This regioselectivity is in sharp contrast to the ortho/para preference that is normally obtained in electrophilic aromatic substitution reactions with toluene. This result implies that resonance stabilization of positive charge by the tolyl group is not of major importance in the transition state for the product-determining step. In the protonation reactions, the inhibition of the isomerization process by the presence of acetonitrile is highly indicative of an associative hydrocarbon/solvent exchange, since the hydrocarbon loss is effectively irreversible on the experimental time scale. A dissociative mechanism is not readily reconciled with either the observed product distributions in the toluene activation or the acetonitrile inhibition of the isomerization processes in the protonation reactions. The unusual selectivities in the C−H activation of toluene and *p*-xylene might be explained by steric and electronic effects for the associative elimination of methane, as will be discussed in the following section.

C−H Activation of Toluene. The most striking aspect of the C−H activation reactions with toluene is the observed meta preference which, to our knowledge, has never been previously reported for this type of reaction. Even after statistical correction for two meta positions vs one para position, meta activation is preferred over para activation by a factor of ca. 2 in the reactions of **1** and **2**. The product ratio corresponds to a relatively small energy difference in the activation barriers that lead to meta and para products. However, the greater than statistical *m*/*p* ratio is consistently seen in our experiments and apparently has not been previously observed in other systems, and in our view deserves special attention.

It is reasonable to assume that the product ratios in these reactions predominantly reflect a *kinetically controlled selectivity*. In agreement with this, a control experiment showed that the activation of toluene at the produced (N^f−N^f)Pt(Tol)(H$_2$O)$^+$ species is considerably slower than the activation at **1** (see Experimental Section). In addition, the C−H activation reactions were quenched by acetonitrile addition once the starting Pt complexes were consumed, as judged by the NMR spectra. This treatment further minimizes the extent to which repeated activation events might take place.

Some additional features of the toluene activation are inferred from the mechanism of the analogous benzene activation reactions at **1** and **2**.[9b,c] Thus, we expect that (1) the interconversion between the hydrocarbon adducts in Scheme 7 is fast compared to the elimination of methane and toluene from these intermediates, and (2) the η^2-C,C- or η^2-C,H-coordinated[27] toluene adduct undergoes facile migration from one C−C/C−H bond to another. The extensive positional isomerization observed in the protonation reactions of the bis(tolyl) species **3a**−**c** in pure TFE clearly supports this scenario. This gives rise to a situation where all the three isomeric (N−N)Pt(Tol)(σ-CH$_4$)$^+$ intermediates (**A**−**C**) are in rapid equilibrium with each other (Figure 4, indicated by the dashed lines). According to the Curtin−Hammett principle, the product distribution will then be determined solely by the differences in the corresponding transition-state energies for the rate-limiting steps that lead to the products. By applying the suggested solvent-assisted associative mechanism for the elimination of methane from the (N−N)Pt(Tol)(σ-CH$_4$)$^+$ intermediates, we propose that the trigonal bipyramidal structures **A**‡−**C**‡ depicted in Figure 4 are reasonable models for the respective transition states. The relative positions of these structures in the energy diagram reflect qualitatively the observed product distributions. In the following, we will elaborate on how our results might be explained by this model.

The relative energies of the ground-state structures **A**−**C** are not known (and, applying the Curtin−Hammett principle, not relevant for the product distribution), but we assume that the ortho isomer **A** is somewhat destabilized relative to the meta (**B**) and para (**C**) isomers due to steric effects. In the transition states, steric interactions between the *o*-tolyl-*Me* group and coordinated methane or TFE in **A**‡ should lead to an even more pronounced destabilization when compared to isomeric structures **B**‡ and **C**‡. This effect provides a straightforward rationale for the nearly complete absence of the *o*-tolyl products **4a** and **5a**. However, steric arguments do not seem to be applicable in

(26) In agreement with rate-limiting hydrocarbon coordination, the activation of trifluoromethylbenzene at **1** was found to be on the order of 10 times slower than the activation of toluene. The identity of the products obtained in this reaction was, however, not determined.

(27) Evidence for a π-coordinated Pt^{II} benzene complex (N′−N′)Pt(CH$_3$)(η^2-C,C-C$_6$H$_6$)$^+$ was recently reported. However, the cleavage of a C−H bond from this species is believed to take place via an η^2-C,H-coordinated benzene intermediate. See ref 9c.

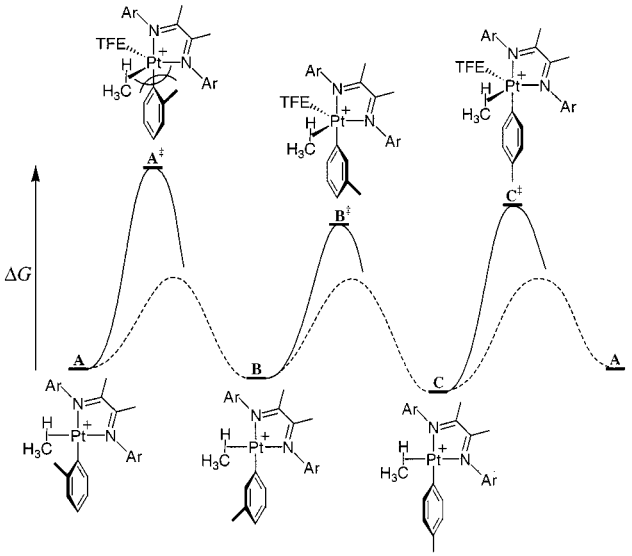

Figure 4. Qualitative reaction coordinate diagram for the reaction path from the square planar (N—N)Pt(Tol)$(CH_4)^+$ intermediates **A**−**C** to the corresponding trigonal bipyramidal transition states **A**‡−**C**‡ according to a TFE-assisted associative mechanism for elimination of methane.

order to account for the required energy difference between **B**‡ and **C**‡. Thus, we have to consider possible electronic effects. In the species in Figure 4, p_π(tolyl)−d_π(Pt) interactions should be present. From simple resonance structure considerations, it may be argued that the *m*-tolyl ligand less efficiently delocalizes the positive charge at Pt than does the *p*-tolyl ligand. This leaves a greater positive charge at Pt in **B** than in **C**, rendering the Pt center of **B** more susceptible to nucleophilic attack. The resonance effect is indicated by a somewhat higher ground-state energy for **B** versus **C** in the diagram. However, for the corresponding transition-state structures **B**‡ and **C**‡, the experimentally observed product distributions dictate that this ordering must be reversed. Two major factors, seemingly working in opposing directions, might be envisioned to govern the relative energies of **B**‡ and **C**‡. Resonance effects will favor structure **C**‡ for the same reason as for the ground-state species **C**, but to a lesser extent because the effective positive charge at Pt is diluted as a consequence of the ligand association. On the other hand, the greater positive charge at Pt in **B**‡ might be predicted to lead to enhanced stabilization due to stronger binding of the electron-donating TFE ligand when compared to **C**‡ in providing a stronger electrostatic component to the bonding of the incoming nucleophile. If this effect is more important, the observed meta preference can, indeed, be rationalized with this model. However, it must be emphasized that the exact explanation for how the electronic effects contribute to the stabilization of **B**‡ versus **C**‡ may be considerably more complicated. We hope to address this point in future contributions.

Importantly, the meta selectivity appears to be in direct conflict with an alternative dissociative mechanism for the elimination of methane. The putative unsaturated three-coordinate intermediates (N—N)Pt(Tol)$^+$ on the reaction coordinate for this pathway should clearly be stabilized by electron-donating ligands. Since the donating capacities for the tolyl ligands decrease in the order *p*-tolyl ≈ *o*-tolyl > *m*-tolyl, an ortho/para preference would be expected if this mechanism were operative.

Romeo and co-workers have investigated in detail the influence of electronic and steric properties on reaction rates and mechanisms for simple ligand exchange processes in square planar Pt^{II} complexes.[28] Their observed trends seem to support the above argumentation. Thus, solvent exchange reactions at (L—L)Pt(CH_3)(DMSO)$^+$ complexes (L—L = chelating diamines and diimines) were generally found to take place by associative mechanisms.[28c] Furthermore, the fastest reactions were observed at the most electron-deficient metal centers. The authors rationalized the fast exchange rates for the electron-poor complexes by (1) high affinity of the metal center for the entering nucleophile and (2) good ability to stabilize a transition state with a higher coordination number. Clear-cut dissociative exchange processes have, on the other hand, been recognized only for electron-*rich* Pt^{II} complexes, in particular with strong *σ*-activators trans to the leaving group, e.g., *cis*-PtR_2L_2 (R = Me, Ph; L = thioethers or DMSO)[28a] and (bph)Pt$(SR_2)_2$ (bph = 2,2′-biphenyl; R = Me, Et).[28d] The electron-rich nature of these complexes has been suggested to promote the changeover from associative to dissociative pathways mainly by (1) thwarting the possibility for nucleophilic attack at the metal centers and (2) enhancing the stability of the corresponding transient three-coordinate, 14-electron Pt^{II} intermediates.[28b]

The apparent lack of meta/para selectivity (after statistical correction) in other C—H activation reactions between toluene and organometallic complexes, as discussed in the Introduction, may well indicate that the product-determining steps in these cases are associated with completely different types of processes, e.g., C—H bond breaking/formation or dissociative alkane loss. Another explanation could be that the present diimine Pt^{II} system is unusually sensitive to electronic effects.

C—H Activation of *p*-Xylene. Whereas the tolyl complexes **4a**−**c** were observed as the exclusive products in the reaction between **1** and toluene, a considerable amount of the benzyl product **5d** was obtained in the reaction of **2**. This difference in selectivity between **1** and **2** became even more prominent in the reactions with *p*-xylene. Thus, the ratios of Pt(xylyl) (**6a**/**7a**) versus Pt(*p*-methylbenzyl) (**6b**/**7b**) products were 90:10 and 7:93 in the reactions with **1** and **2**, respectively. This remarkable diversity in selectivity is most likely a result of differences in the steric influence from the diimine ligands in **1** and **2**.

If we assume that the mechanistic model that was utilized in the discussion about the toluene reaction still applies (i.e. rapidly equilibrating isomeric Pt^{II} *p*-xylene adduct intermediates), the product-determining factors might once again be found in the trigonal bipyramidal transition-state structures (Figure 5). For the reaction with **1**, the product distribution implies that that the energy for transition state **D**‡ is lower than that for **E**‡. The reasons for this may be that (1) M—C(sp^2) bonds in general are stronger than M—C(sp^3) bonds and (2) the positive charge at Pt is stabilized by resonance. Steric interactions, which should favor structure **E**‡, appear to be of lesser importance.

In contrast, the reaction of complex **2** led to almost exclusive C—H activation of the *p*-xylene methyl groups. This finding is most readily rationalized by the steric properties of the diimine ligand in **2**. Steric repulsions between the diimine aryl 2,6-*Me* groups and the *o*-tolyl-*Me* substituent lead to a significant destabilization of the transition-state structure **F**‡ (Figure 5). Consequently, product formation via the less crowded transition-state structure **G**‡ becomes the dominant pathway. By analogy, the same effects explain the observation of considerable amounts of benzylic product in the reaction between **2** and toluene.

The above argumentation is based on the assumption that the equilibration of all involved intermediates is fast compared

(28) (a) Frey, U.; Helm, L.; Merbach, A. E.; Romeo, R. *J. Am. Chem. Soc.* **1989**, *111*, 8161. (b) Romeo, R.; Grassi, A.; Scolaro, L. M. *Inorg. Chem* **1992**, *31*, 4383. (c) Romeo, R.; Scolaro, L. M.; Nastasi, N.; Arena, G. *Inorg. Chem.* **1996**, *35*, 5087. (d) Plutino, M. R.; Scolaro, L. M.; Romeo, R.; Grassi, A. *Inorg. Chem.* **2000**, *39*, 2712.

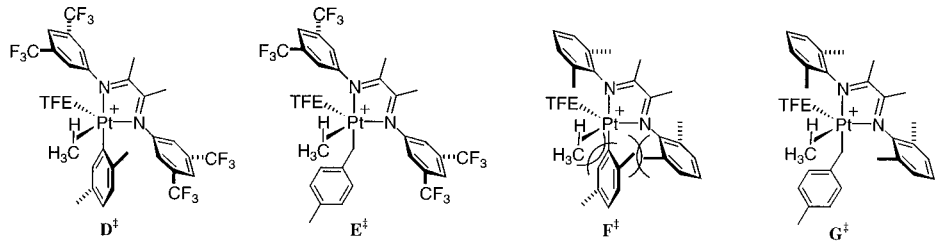

Figure 5. Proposed transition-state structures for the displacement of methane by TFE during the C−H activation reactions of *p*-xylene at **1** (**D**‡, **E**‡) and **2** (**F**‡, **G**‡).

Scheme 8

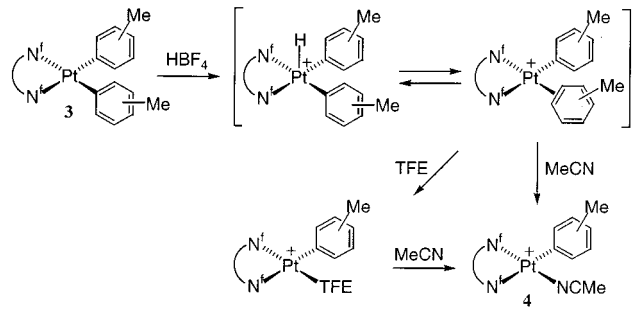

to methane loss—i.e., that coordinated toluene and *p*-xylene molecules are capable of rapidly rearranging between the "aromatic" and "benzylic" C−H bond coordination modes. This scenario is, indeed, supported by the observation of significant amounts of the benzyl product (N′−N′)Pt(Bz)(NCMe)$^+$ (**5d**) arising from the protonation of the bis(*p*-tolyl) complex **9c** in the presence of 0.05 M MeCN in TFE. If, alternatively, the aromatic/benzylic coordination rearrangement is slow compared to elimination of methane in the C−H activation reactions, then initial hydrocarbon coordination must control the discrimination between aromatic versus benzylic activation. However, since the transition-state structures for the coordination of toluene and *p*-xylene at the starting platinum species **1** and **2** will be analogous to those depicted in Figure 5 (with CH_4 and xylyl/*p*-methylbenzyl ligands being replaced by *p*-xylene and methyl, respectively), an extrapolation of the steric arguments above will lead to similar explanations for the observed selectivities.

Protonation Reactions. Protonolysis of the three bis(tolyl) complexes **3a**−**c** in neat TFE led to extensive positional isomerization (Table 5). In analogy with the H/D scrambling observed in the activation reactions with deuterated methane and benzene,[9b,c] this is straightforwardly explained by a rapid equilibrium between (N^f—N^f)Pt^{IV}(Tol)$_2$(H)$^+$ and (N^f—N^f)Pt^{II}(Tol)(toluene)$^+$ intermediates (Scheme 8). In addition, fast rearrangement of toluene between different η^2-C,H- and η^2-C,C-coordination modes in (N^f—N^f)Pt^{II}(Tol)(toluene)$^+$ must take place. The elimination of toluene may be confidently assumed to be irreversible under these conditions since (1) the reaction between toluene and the (N^f—N^f)Pt(Tol)(H$_2$O)$^+$ products is slow (vide supra), (2) the reaction times were short (ca. 5 min) and the products were irreversibly trapped by acetonitrile addition prior to analysis, and (3) toluene is present only in low concentrations throughout the reactions.

The products **4b** and **4c** were obtained in a 77:23 ratio in all experiments performed in neat TFE, regardless of which bis(tolyl) complex **3a**−**c** was protonated. This product distribution must therefore reflect the true kinetic selectivity of toluene elimination when the isomeric intermediates within the brackets in Scheme 8 are at equilibrium. This is again a situation where the Curtin−Hammett principle applies, and consequently, the transition-state energies for elimination of toluene from the isomeric (N^f—N^f)Pt(Tol)(toluene)$^+$ species increase in the order (N^f—N^f)Pt(*m*-Tol)(toluene)$^+$ < (N^f—N^f)Pt(*p*-Tol)(toluene)$^+$ ≪ (N^f—N^f)Pt(*o*-Tol)(toluene)$^+$. This is entirely analogous to the trend for elimination of methane from the putative (N^f—N^f)Pt(Tol)(CH$_4$)$^+$ intermediates in the toluene activation reaction at **1**. Again, the results appear incompatible with a dissociative mechanism since the most facile toluene elimination takes place from the meta intermediate, which is presumably least capable of stabilizing the positive charge. The total absence of *o*-tolyl product in the protonation reactions implies that the five-coordinate transition-state structure [(N^f—N^f)Pt(*o*-Tol)(toluene)(TFE)$^+$]‡ is even more unfavorable relative to the *m*- and *p*-tolyl analogues than was the case for [(N^f—N^f)Pt(*o*-Tol)(CH$_4$)(TFE)$^+$]‡ (cf. Figure 4). Since toluene is considerably larger than methane, this difference may be attributed to enhanced steric effects in the corresponding transition states for elimination of toluene when compared to methane.

In the presence of 1.7 M acetonitrile, considerably less isomerization is seen in the reactions. This indicates that acetonitrile, which is a considerably better incoming nucleophile and coordinating ligand than TFE, displaces toluene at platinum *before* complete equilibriation of the intermediates has been established. This result strongly indicates that the toluene/acetonitrile exchange also occurs in an associative fashion.

In neat acetonitrile, protonation of **3b** gives no positional isomerization, and only traces of isomerization occur in the reaction of **3c**. Contrary to this, the protonation of **3a** led to extensive isomerization—only 7% of the product mixture was identified as the corresponding *o*-tolyl product **4a**. From these observations it is evident that (1) the extent of isomerization is *dependent* on the acetonitrile concentration and (2) the elimination of toluene from the sterically most congested metal center, (N^f—N^f)Pt(*o*-Tol)(toluene)$^+$, is highly *unfavorable* when compared to the isomeric meta and para intermediates. Once again, these results appear to be in conflict with a dissociative mechanism for the toluene elimination and provide further support for the proposed associative pathway for this process.

Concluding Remarks

The cationic aqua complexes **1** and **2** undergo facile C−H activation of toluene and *p*-xylene in TFE at ambient temperature. Analysis of the product mixtures obtained in these reactions and mechanistic insight gained from the study on the elimination of toluene through protonolysis of the bis(tolyl) complexes **3a**−**c** and **9c** have allowed us to address several important questions regarding the factors that govern regioselectivity in these systems.

The selectivity in the C−H activation appears to be dictated by the following key mechanistic features: (1) a *rapid* dynamic equilibrium between the isomeric (N−N)Pt(Ar)(CH$_4$)$^+$ intermediates (Ar = tolyl/benzyl or xylyl/*p*-methylbenzyl) precedes (2) a relatively *slow* exchange of TFE or H$_2$O for methane from these species by (3) an *associative* mechanism. Items (1) and

(2) imply that the presumed rate-determining step, coordination of the arene, does *not* affect the selectivity in the reactions. Another consequence is that differences in C—H bond strengths within the hydrocarbon substrates are irrelevant for the C—H activation selectivity.[29] Most importantly, (3) implies that the product-determining factors are found in the pentacoordinate transition-state structures $[(N{-}N)Pt(Ar)(CH_4)(TFE)^+]^‡$ for the elimination of methane. Steric as well as electronic effects influence the relative stabilities of these structures.

The observed selectivity order for the aromatic positions in the toluene activation, meta > para > ortho, appears incompatible with the alternative dissociative mechanism for the product-determining step. According to our mechanistic model, the disfavored formation of *o*-tolyl products is explained by steric destabilization of the corresponding transition-state structure $[(N{-}N)Pt(o\text{-}Tol)(CH_4)(TFE)^+]^‡$. The meta over para preference is, on the other hand, caused largely by electronic effects. Thus, the poorer capacity of the *m*-tolyl versus the *p*-tolyl ligand to disperse the positive charge at Pt is proposed to lead to enhanced bonding of the incoming TFE ligand.

Differences in the steric influences from the diimine ligands in **1** and **2** have dramatic consequences for the selectivity in the reactions with *p*-xylene. By utilizing the same mechanistic model as for the toluene activation reaction, the selectivities are again explained by the relative energies for the corresponding transition-state structures for the associative methane elimination processes to the products.

In more general terms, the results illuminate an important aspect of product formation by reductive elimination from X—M—Y species. Product distributions in such reactions are commonly discussed in terms of the driving force as measured by X—Y bond strengths in the alternative products. The present examples show that this factor may be of subordinate importance in cases where associative displacement of the coordinated X—Y molecule is rate-determining. It remains to be seen whether effects similar to those described in this paper contribute to determine the selectivity in alkane activation and functionalization reactions in Shilov-type systems.

Experimental Section

General Considerations. Trifluoroethanol (TFE) and TFE-d_3 were distilled from $CaSO_4$ and a small amount of $NaHCO_3$ and stored over 3-Å molecular sieves. All other solvents were purified according to standard procedures. ^{1}H, ^{13}C{^{1}H}, and ^{19}F NMR spectra were recorded on Bruker Advance DXP 200 and 300 instruments. ^{1}H and ^{13}C chemical shifts are reported in ppm relative to tetramethylsilane, with the residual solvent proton resonance as internal standards. ^{19}F chemical shifts are reported in ppm relative to $CFCl_3$. For TFE-d_3, the solvent fluorine resonance was used as internal standard (δ −77.72). Elemental analyses were carried out at Ilse Beetz Mikroanalytisches Laboratorium, Kronach, Germany. The preparation of the diimine ligands $N^f{-}N^f$ [9a] and N′—N′ [30] as well as the aqua complexes **1**(BF_4^-)[9a] and **2**(BF_4^-)[9c] is described elsewhere. $PtCl_2(SMe_2)$,[21] *cis*-Pt(*m*-Tol)$_2$(SMe$_2$)$_2$,[22a] and *cis*-Pt(*p*-Tol)$_2$(SMe$_2$)$_2$[22b] were prepared by methods similar to those described in the literature.

***cis*-Pt(*o*-Tol)$_2$(SMe$_2$)$_2$.** The complex was prepared by adaptation of the reported synthesis for *cis*-Pt(*m*-Tol)$_2$(SMe$_2$)$_2$[22a] (39%, obtained as a mixture of two isomers, tentatively proposed to be the *syn*-(*cis*-Pt(*o*-Tol)$_2$(SMe$_2$)$_2$) and *anti*-(*cis*-Pt(*o*-Tol)$_2$(SMe$_2$)$_2$) complexes). ^{1}H NMR (200 MHz, dichloromethane-d_2): major isomer (64%), δ 2.06 (s, $^3J(^{195}Pt{-}H)$ = 24.6 Hz, 12 H, S*Me*$_2$), 2.67 (s, $^4J(^{195}Pt{-}H)$ = 7.3 Hz, 6 H, Tol*Me*), 6.66−6.93 (m, 6 H, TolH_m and TolH_p), 6.97 ("dd", ^3J(H—H) = 7.0 Hz, $^3J(^{195}Pt{-}H)$ = 73.2 Hz, 2 H, TolH_o); minor isomer (36%), δ 2.08 (s, $^3J(^{195}Pt{-}H)$ = 24.2 Hz, 12 H, S*Me*$_2$), 2.57 (s, $^4J(^{195}Pt{-}H)$ = 6.9 Hz, 6 H, Tol*Me*), 6.66−6.93 (overlap with major isomer, 6 H, TolH_m and TolH_p), 6.97 (overlap with major isomer, 2 H, TolH_o).

General Procedure for the Preparation of Complexes ($N^f{-}N^f$)-Pt(Tol)$_2$ (3a−c) and (N′—N′)Pt(*p*-Tol)$_2$ (9c). One equivalent of the diimine ligand $N^f{-}N^f$ or N′—N′ was added to a solution of the appropriate Pt(Tol)$_2$(SMe$_2$)$_2$ complex in toluene. The solution was stirred at 45 °C overnight. The solvent was removed, and the residue was recrystallized from a dichloromethane/pentane mixture. The product was obtained after drying in vacuo.

***syn*-($N^f{-}N^f$)Pt(*o*-Tol)$_2$ (*syn*-3a) and *anti*-($N^f{-}N^f$)Pt(*o*-Tol)$_2$ (*anti*-3a).** This compound was prepared from *cis*-Pt(*o*-Tol)$_2$(SMe$_2$)$_2$ (482 mg, 0.961 mmol) and the diimine ligand $N^f{-}N^f$ (489 mg, 0.962 mmol) in toluene (50 mL). Dark purple microcrystals formed (720 mg, 85%). ^{1}H NMR (200 MHz, dichloromethane-d_2): *syn*-**3a** (54%), δ 1.71 (s, 6 H, NC(*Me*)C(*Me*)N), 2.31 (s, $^4J(^{195}Pt{-}H)$ = 6.7 Hz, 6 H, Tol*Me*), 6.34−6.66 (m, 6 H, TolH_m and TolH_p), 6.90 ("d", ^3J(H—H) = 7.5 Hz, $^3J(^{195}Pt{-}H)$ = 76.8 Hz, 2 H, TolH_o), 7.17 (s, 2 H, ArH_o), 7.37 (s, 2 H, ArH_o′), 7.58 (s, 2 H, ArH_p); *anti*-**3a** (46%), δ 1.71 (s, 6 H, NC(*Me*)C(*Me*)N), 2.13 (s, $^4J(^{195}Pt{-}H)$ = 6.4 Hz, 6 H, Tol*Me*)), 6.34−6.66 (m, 6 H, TolH_m and TolH_p), 7.04 ("d", ^3J(H—H) = 8.0 Hz, $^3J(^{195}Pt{-}H)$ = 70.5 Hz, 2 H, TolH_o), 7.28 (s, 4 H, ArH_o), 7.56 (s, 2 H, ArH_p). ^{19}F NMR (188 MHz, dichloromethane-d_2): *syn*-**3a**, δ −62.98 (s, 6 F, ArCF_3) −62.85 (s, 6 F ArCF_3′); *anti*-**3a**, δ −63.35 (s, 12 F, ArCF_3). Anal. Calcd for $C_{34}H_{26}F_{12}N_2Pt$: C, 46.11; H, 2.96; N, 3.16. Found: C, 44.26; H, 3.12; N, 2.98.

($N^f{-}N^f$)Pt(*m*-Tol)$_2$ (3b). This compound was prepared from *cis*-Pt(*m*-Tol)$_2$(SMe$_2$)$_2$ (121 mg, 0.241 mmol) and the diimine ligand $N^f{-}N^f$ (123 mg, 0.242 mmol) in toluene (15 mL). Dark purple microcrystals formed (179 mg, 84%). ^{1}H NMR (300 MHz, dichloromethane-d_2): δ 1.81 (s, 6 H, NC(*Me*)C(*Me*)N), 1.89 (s, 6 H, Tol*Me*), 6.30 ("d", ^3J(H—H) = 7.3 Hz, 2 H, TolH_p), 6.49 ("dd", ^3J(H—H) = 7.3 Hz, 2 H, TolH_m), 6.53 (s, $^3J(^{195}Pt{-}H)$ = 72.0 Hz, 2 H, TolH_o), 6.55 ("d", ^3J(H—H) = 7.3 Hz, $^3J(^{195}Pt{-}H)$ = 72.9 Hz, 2 H, TolH_o′), 7.25 (s, 4 H, ArH_o), 7.60 (s, 2 H, ArH_p).^{19}F NMR (188 MHz, dichloromethane-d_2): δ −63.10 (s, ArCF_3). Anal. Calcd for $C_{34}H_{26}F_{12}N_2Pt$: C, 46.11; H, 2.96; N, 3.16. Found: C, 46.47; H, 3.14; N, 3.51.

($N^f{-}N^f$)Pt(*p*-Tol)$_2$ (3c). This compound was prepared from *cis*-Pt(*p*-Tol)$_2$(SMe$_2$)$_2$ (448 mg, 0.893 mmol) and the diimine ligand $N^f{-}N^f$ (455 mg, 0.895 mmol) in toluene (60 mL). Dark purple microcrystals formed (791 mg, 82%). ^{1}H NMR (200 MHz, dichloromethane-d_2): δ 1.79 (s, 6 H, NC(*Me*)C(*Me*)N), 2.04 (s, 6 H, Tol*Me*), 6.42 ("d", ^3J(H—H) = 8.0 Hz, 4 H, TolH_m), 6.53 ("d", ^3J(H—H) = 7.3 Hz, $^3J(^{195}Pt{-}H)$ = 73.7 Hz, 4 H, TolH_o), 7.24 (s, 4 H, ArH_o), 7.61 (s, 2 H, ArH_p).^{19}F NMR (188 MHz, dichloromethane-d_2): δ −63.28 (s, ArCF_3). Anal. Calcd for $C_{34}H_{26}F_{12}N_2Pt$: C, 46.11; H, 2.96; N, 3.16. Found: C, 46.65; H, 3.15; N, 3.56.

(N′—N′)Pt(*p*-Tol)$_2$ (9c). This compound was prepared from *cis*-Pt(*p*-Tol)$_2$(SMe$_2$)$_2$ (193 mg, 0.385 mmol) and the diimine ligand N′—N′ (113 mg, 0.386 mmol) in toluene (20 mL). Dark purple powder formed (229 mg, 89%). ^{1}H NMR (300 MHz, dichloromethane-d_2): δ 1.60 (s, 6 H, NC*Me*C*Me*N), 1.99 (s, 6 H, Tol*Me*), 2.19 (s, 12 H, Ar*Me*), 6.33 ("d", ^3J(H—H) = 7.9 Hz, 4 H, TolH_m), 6.68 ("d", ^3J(H—H) = 7.9 Hz, $^3J(^{195}Pt{-}H)$ = 70.1 Hz, 4 H, TolH_o), 6.85−6.94 (m, 6 H, Ar*H*). Anal. Calcd for $C_{34}H_{38}N_2Pt$: C, 60.97; H, 5.72; N, 4.18. Found: C, 61.11; H, 5.59; N, 4.21.

($N^f{-}N^f$)Pt(*o*-Tol)(Cl) (8). A 1.0 M solution of HCl in diethyl ether (0.65 mL, 0.65 mmol) was added with a syringe to a solution of *cis*-Pt(*o*-Tol)$_2$(SMe$_2$)$_2$ (308 mg, 0.613 mmol) in dichloromethane (40 mL). The mixture was stirred for 1 h. The solvent was removed, and the solid was washed with cold diethyl ether portions. According to ^{1}H NMR spectroscopy, this material consisted of a complex mixture of products, presumably *cis*-Pt(Cl)(*o*-Tol)(SMe$_2$)$_2$, *trans*-Pt(Cl)(*o*-Tol)-(SMe$_2$)$_2$, *cis*-Pt$_2$(Cl)$_2$(*o*-Tol)$_2$(μ-SMe$_2$)$_2$, and *trans*-Pt$_2$(Cl)$_2$(*o*-Tol)$_2$(μ-SMe$_2$)$_2$. This material (271 mg) and the diimine ligand $N^f{-}N^f$ (312 mg, 0.614 mmol) were dissolved in toluene (40 mL), and the mixture was stirred at 70 °C for 14 h. The solvent was removed, and the ^{1}H

(29) The fact that the selectivity cannot be predicted from the substrate C—H bond strengths appears to be a general feature of the majority of nonradical hydrocarbon C—H activation reactions with metal complexes. However, since various mechanisms seem to operate in different C—H activation reactions, there is probably not a general explanation for this behavior. See refs 2 and 20 and references therein.

(30) tom Dieck, H.; Svoboda, M.; Grieser, T. *Z. Naturforsch.* **1981**, *36B*, 823.

NMR spectrum of the solid material revealed a mixture of **8**, *trans*-Pt(Cl)(*o*-Tol)(SMe_2)$_2$, and N^f—N^f ligand in approximately a 1:1:1 ratio. The mixture was separated by flash chromatography (silica/dichloromethane), and **8** was collected as the first dark red fraction. The solvent was removed, and the product was washed with pentane and dried in vacuo, giving a dark red powder (235 mg, 46%).^{1}H NMR (200 MHz, dichloromethane-d_2): δ 1.43 (s, $^4J(^{195}\text{Pt—H}) = 10.5$ Hz, 3 H, NC*Me*C′MeN), 2.02 (s, 3 H, NCMeC′*Me*N), 2.26 (s, $^4J(^{195}\text{Pt—H}) = 7.0$ Hz, 3 H, Tol*Me*), 6.42−6.56 ("m", 3 H, TolH_m, TolH_m′, TolH_p), 6.82 ("m", $^3J(^{195}\text{Pt—H}) = 35$ Hz, 1 H, TolH_o), 7.24 (s, 2 H, ArH_o), 7.56 (s, 1 H, ArH_p), 7.72 (s, 2 H, Ar′H_o), 7.95 (s, 1 H, Ar′H_p). ^{19}F NMR (188 MHz, dichloromethane-d_2): δ −63.55 (s, 3 F, ArCF_3), −63.21 (s, 3 F, ArCF_3′), −63.02 (s, 6 F, Ar′CF_3).

(N^f—N^f)Pt(*o*-Tol)(NCMe)$^+$OTf$^-$ (4a(OTf$^-$)). Solid AgOTf (20 mg, 0.077 mmol) was added to a solution of **8** (62 mg, 0.075 mmol) in THF (10 mL) and acetonitrile (3 mL). After being stirred for 20 min, the mixture was filtered, and the solvent was removed. The oily residue was dissolved in a small amount of diethyl ether, and pentane was added to the solution. After the solution was cooled to −20 °C, the product precipitated as orange needles (54 mg, 74%). ^{1}H NMR (200 MHz, dichloromethane-d_2): δ 2.08 (s, 3 H, $^4J(^{195}\text{Pt—H}) = 14.0$ Hz, PtNC*Me*), 2.23 (s, $^4J(^{195}\text{Pt—H}) = 9.1$ Hz, 3 H, NC*Me*C′MeN), 2.37 (s, 3 H, NCMeC′*Me*N), 2.37 (s, 3 H, Tol*Me*), 6.5−6.6 ("m", 3 H, TolH_m, TolH_m′, TolH_p), 6.82 ("m", $^3J(^{195}\text{Pt—H}) = 37$ Hz, 1 H, TolH_o), 7.44 (s, 1 H, ArH_o), 7.47 (s, 1 H, ArH_o′), 7.55 (s, 1 H, ArH_p), 7.99 (s, 1 H, Ar′H_p), 8.03 (s, 2 H, Ar′H_o). ^{19}F NMR (188 MHz, dichloromethane-d_2): δ −78.70 (s, 3 F, CF_3SO$_3^-$), −63.58 (s, 3 F, ArCF_3), −63.24 (s, 3 F, ArCF_3′), −62.93 (s, 6 F, Ar′CF_3). Anal. Calcd for $C_{30}H_{22}BF_{15}N_3O_3PtS$: C, 36.59; H, 2.25; N, 4.27. Found: C, 37.00; H, 2.78; N, 4.38.

(N^f—N^f)Pt(*m*-Tol)(NCMe)$^+$BF$_4^-$ (4b(BF$_4^-$)). A 54% solution of HBF_4 in ether (14 μL, 0.10 mmol) was added with a syringe to a solution of **3b** (87 mg, 0.098 mmol) in acetonitrile (15 mL). The mixture was stirred for 20 min. The solvent was removed, and the solid was washed with diethyl ether portions and dissolved in a minimum amount of acetone. The product was obtained as an orange powder (80 mg, 88%) by the addition of diethyl ether. ^{1}H NMR (200 MHz, dichloromethane-d_2): δ 1.96 (s, 3 H, Tol*Me*), 2.09 (s, 3 H, $^4J(^{195}\text{Pt—H}) = 13.5$ Hz, PtNC*Me*), 2.25 (s, $^4J(^{195}\text{Pt—H}) = 9.3$ Hz, 3 H, NC*Me*C′MeN), 2.36 (s, 3 H, NCMeC′*Me*N), 6.4−6.6 (m, 4 H, Tol*H*), 7.39 (s, 2 H, ArH_o), 7.60 (s, 1 H, ArH_p), 7.96 (s, 2 H, Ar′H_o), 7.99 (s, 1 H, Ar′H_p). ^{19}F NMR (188 MHz, dichloromethane-d_2): δ −150.39 (s, 4 F, BF_4^-), −63.22 (s, 6 F, ArCF_3), −62.95 (s, 6 F, Ar′CF_3). Anal. Calcd for $C_{29}H_{22}BF_{16}N_3Pt$: C, 37.76; H, 2.40; N, 4.56. Found: C, 38.14; H, 2.51; N, 4.34.

(N^f—N^f)Pt(*p*-Tol)(NCMe)$^+$BF$_4^-$ (4c(BF$_4^-$)). A 54% solution of HBF_4 in ether (20 μL, 0.15 mmol) was added with a syringe to a solution of **3c** (125 mg, 0.141 mmol) in acetonitrile (15 mL). The mixture was stirred for 20 min. The solvent was removed, and the solid was washed with diethyl ether portions and dissolved in a minimum amount of acetone. The product was obtained as an orange powder (130 mg, 85%) by the addition of diethyl ether. ^{1}H NMR (200 MHz, dichloromethane-d_2): δ 2.09 (s, 3 H, Tol*Me*), 2.09 (s, 3 H, $^4J(^{195}\text{Pt—H}) = 13.8$ Hz, PtNC*Me*), 2.25 (s, $^4J(^{195}\text{Pt—H}) = 9.3$ Hz, 3 H, NC*Me*C′MeN), 2.36 (s, 3 H, NCMeC′*Me*N), 6.50 ("m", 2 H, TolH_m), 6.57 ("m", $^3J(^{195}\text{Pt—H}) = 35.2$ Hz, 2 H, TolH_o), 7.37 (s, 2 H, ArH_o), 7.61 (s, 1 H, ArH_p), 7.96 (s, 2 H, Ar′H_o), 8.00 (s, 1 H, Ar′H_p). ^{19}F NMR (188 MHz, dichloromethane-d_2): δ −150.40 (s, 4 F, BF_4^-), −63.45 (s, 6 F, ArCF_3), −62.94 (s, 6 F, Ar′CF_3). Anal. Calcd for $C_{29}H_{22}BF_{16}N_3Pt$: C, 37.76; H, 2.40; N, 4.56. Found: C, 38.15; H, 2.55; N, 4.35.

General Procedure for the Reactions between 1/2 and Toluene/*p*-Xylene. The aromatic substrate (ca. 0.24 mmol, 0.4 M) was added to a solution of **1**(BF$_4^-$) or **2**(BF$_4^-$) (ca. 8×10^{-3} mmol) in TFE-d_3 (0.6 mL) in an NMR tube. The reactions were followed by ^{1}H NMR spectroscopy. After complete conversion to the products, acetonitrile was added to the solution. The solvent was removed, and the residue was dissolved in dichloromethane-d_2. The product mixtures were analyzed by NMR spectroscopy.

Reaction between 1 and Toluene. The ^{1}H and ^{19}F NMR spectra showed a product mixture consisting of **4a** (9%), **4b** (70%), and **4c** (21%).

Reaction between 2 and Toluene. The ^{1}H NMR spectrum showed a product mixture consisting of (N′—N′)Pt(*o*-Tol)(NCMe)$^+$ (**5a**, 4%), (N′—N′)Pt(*m*-Tol)(NCMe)$^+$ (**5b**, 60%), (N′—N′)Pt(*p*-Tol)(NCMe)$^+$ (**5c**, 15%), and (N′—N′)Pt($CH_2C_6H_5$)(NCMe)$^+$ (**5d**, 21%). ^{1}H NMR (300 MHz, dichloromethane-d_2): **5a** (characteristic signals), δ 1.86 (s, $^4J(^{195}\text{Pt—H}) = 13$ Hz, 3 H, PtNC*Me*), 2.01 (s, 3 H, Ar*Me*), 2.11 (s, 3 H, NC*Me*C′MeN), 2.22 (s, 3 H, NCMeC′*Me*N), 2.32 (s, 3 H, Ar*Me*), 2.37 (s, 3 H, Ar*Me*) 2.45 (s, $^4J(^{195}\text{Pt—H}) = 6$ Hz, 3 H, Tol*Me*), 2.47 (s, 3 H, Ar*Me*) [The observation of four separate Ar*Me* signals for this species indicates that rotation of *both* the diimine aryl groups around the N—C_{Aryl} axes is restricted.]; **5b**, δ 1.88 (s, $^4J(^{195}\text{Pt—H}) = 13$ Hz, 3 H, PtNC*Me*), 1.96 (s, 3 H, Tol*Me*), 2.11 (s, 3 H, $^4J(^{195}\text{Pt—H}) = 9.4$ Hz, NC*Me*C′MeN), 2.16 (s, 6 H, Ar*Me*), 2.21 (s, 3 H, NCMeC′*Me*N), 2.40 (s, 6 H, Ar′*Me*), 6.4−6.6 (m, 4 H, Tol*H*), 6.9−7.0 (m, 3 H, Ar*H*) 7.2−7.3 (m, 3 H, Ar′*H*); **5c** (characteristic signals), δ 1.87 (s, 3 H, PtNC*Me*), 2.08 (s, 3 H, Tol*Me*), 2.10 (s, 3 H, NC*Me*C′MeN), 2.16 (s, 6 H, Ar*Me*), 2.20 (s, 3 H, NCMeC′*Me*N), 2.40 (s, 6 H, Ar′*Me*); **5d** (characteristic signals), δ 1.67 (s, $^4J(^{195}\text{Pt—H}) = 13.9$ Hz, 3 H, PtNC*Me*), 2.04 (s, 3 H, NC*Me*C′MeN), 2.08 (s, 3 H, NCMeC′*Me*N), 2.22 (s, 6 H, Ar*Me*), 2.28 (s, 6 H, Ar′*Me*), 2.68 (s, $^2J(^{195}\text{Pt—H}) = 102.0$ Hz, 3 H, PtCH_2), 6.75 (m, 2 H, PtCH_2PhH_o).

Reaction between 1 and *p*-Xylene. The ^{1}H and ^{19}F NMR spectra showed a product mixture consisting of (N^f—N^f)Pt(Xyl)(NCMe)$^+$ (**6a**, 93%) and (N^f—N^f)Pt(*p*-MeBz)(NCMe)$^+$ (**6b**, 7%). ^{1}H NMR (300 MHz, dichloromethane-d_2): **6a**, δ 1.96 (s, 3 H, XylMe_m), 2.08 (s, $^4J(^{195}\text{Pt—H}) = 13.8$ Hz, 3 H, PtNC*Me*), 2.21 (s, 3 H, NC*Me*C′MeN), 2.34 (s, 3 H, XylMe_o), 2.35 (s, 3 H, NCMeC′*Me*N), 6.38 and 6.43 ("d", $^3J(\text{H—H}) = 7.7$ Hz, 1 H each, XylH_m and XylH_p), 6.59 (s, $^3J(^{195}\text{Pt—H}) = 32.7$ Hz, 1 H, XylH_o), 7.38 (s, 1 H, ArH_o), 7.41 (s, 1 H, ArH_o′), 7.56 (s, 1 H, ArH_p), 7.96 (s, 2 H, Ar′H_o), 8.00 (s, 1 H, Ar′H_p); **6b** (characteristic signals), δ 1.81 (s, 3 H, PtNC*Me*), 2.78 (s, $^2J(^{195}\text{Pt—H}) = 101.9$ Hz, 3 H, PtCH_2), 6.76 (d, $^3J(\text{H}_a\text{—H}_b) = 7.7$ Hz, 2 H, *p*-MeBzH_a), 6.80 (d, $^3J(\text{H}_a\text{—H}_b) = 7.7$ Hz, 2 H, *p*-MeBzH_b). ^{19}F NMR (188 MHz, dichloromethane-d_2): **6a**, δ −150.19 (s, 4 F, BF_4^- counterion), −63.50 (s, 3 F, ArCF_3), −62.95 (s, 3 F, ArCF_3′), −62.92 (s, 6 F, Ar′CF_3); **6b**, δ −150.19 (s, 4 F, BF_4^- counterion), −63.14 (s, 6 F, ArCF_3), −63.00 (s, 6 F, Ar′CF_3).

Reaction between 2 and *p*-Xylene. The ^{1}H and ^{19}F NMR spectra showed a product mixture consisting of (N′—N′)Pt(Xyl)(NCMe)$^+$ (**7a**, 10%) and (N′—N′)Pt(*p*-MeBz)(NCMe)$^+$ (**7b**, 90%). ^{1}H NMR (300 MHz, dichloromethane-d_2): **7a** (characteristic signals), δ 1.86 (s, $^4J(^{195}\text{Pt—H}) = 13.7$ Hz, 3 H, PtNC*Me*), 1.97 (s, 3 H, XylMe_m), 2.11 (s, 3 H, NC*Me*C′MeN), 2.20 (s, 3 H, NCMeC′*Me*N), 2.46 (s, 3 H, XylMe_o), 6.27 (s, $^3J(^{195}\text{Pt—H}) = 33.4$ Hz, 1 H, XylH_m), 6.37 and 6.53 (d, $^3J(\text{H}_a\text{—H}_b) = 7.6$ Hz, 1 H each, XylH_m and XylH_p), 6.73 (d, $^3J(\text{H}_a\text{—H}_b) = 7.6$ Hz, 1 H, ArH_m), 6.94 ("t", $^3J(\text{H}_a\text{—H}_b) = 7.6$ Hz, 1 H, ArH_p), 7.08 (d, $^3J(\text{H}_a\text{—H}_b) = 7.6$ Hz, 1 H, ArH_m′) [The three latter signals are assigned to the diimine aryl ring neighboring the xylyl ligand; the observation of two separate ArH_m signals suggests that rotation around the N—C_{Ar} axis is restricted, cf. complex **5a**.]; **7b**, δ 1.68 (s, $^4J(^{195}\text{Pt—H}) = 13.9$ Hz, 3 H, PtNC*Me*), 2.02 (s, $^4J(^{195}\text{Pt—H}) = 9.2$ Hz, 3 H, NC*Me*C′MeN), 2.07 (s, 3 H, NCMeC′*Me*N), 2.12 (s, 3 H, *p*-*Me*Bz), 2.21 (s, 6 H, Ar*Me*), 2.27 (s, 6 H, Ar′*Me*), 2.63 (s, $^2J(^{195}\text{Pt—H}) = 101.4$ Hz, 3 H, PtCH_2), 6.62 (d, $^3J(\text{H}_a\text{—H}_b) = 7.8$ Hz, 2 H, *p*-MeBzH_a), 6.80 (d, $^3J(\text{H}_a\text{—H}_b) = 7.7$ Hz, 2 H, *p*-MeBzH_b), 7.14−7.24 (m, 3 H, Ar*H*), 7.29 (m, 3 H, Ar′*H*).

General Procedure for the Protonation of (N^f—N^f)Pt(Tol)$_2$ Complexes (3a−c) and (N′—N′)Pt(*p*-Tol)$_2$ (9c). Three round-bottomed flasks were loaded with the appropriate (N^f—N^f)Pt(Tol)$_2$ species (10 mg, 0.011 mmol). Three mixtures of a 48% aqueous solution of HBF_4 (1.6 μL, 0.012 mmol) in TFE (5.0 mL), TFE (5.0 mL)/acetonitrile (500 μL), or acetonitrile (5.0 mL), respectively, were then added to the flasks. The reaction mixtures were stirred until all the starting material had reacted to give orange product solutions (ca. 5 min). Acetonitrile (500 μL) was added to the reaction that was performed in neat TFE. The solvent was removed in vacuo, and the resulting materials were dissolved in dichloromethane-d_2 and analyzed by ^{1}H and ^{19}F NMR spectroscopy. The protonation of **9c** in 0.05 M acetonitrile in TFE was performed in a similar manner.

Examination of the Rates for Toluene Activation at 1 versus Mixture of Isomeric (N^f—N^f)Pt(Tol)(H$_2$O)$^+$ Complexes. Toluene (16

μL, 0.15 mmol) was added to an NMR tube loaded with **1** (4.1 mg, 5.0 μmol) dissolved in TFE-d_3 (600 μL). After 65 min at 25 °C, the ^{1}H NMR spectrum showed that ca. 95% of **1** had reacted to $(N^f{-}N^f)Pt(Tol)(H_2O)^+$ products and CH_4. The reaction was allowed to proceed for an additional hour, and the solvent was removed in vacuo. The resulting mixture of $(N^f{-}N^f)Pt(Tol)(H_2O)^+$ species was dissolved in TFE-d_3 (600 μL), and the solution was transferred to an NMR tube. Toluene-d_8 (16 μL, 0.15 mmol) was added to the tube, and the following reaction was followed by ^{1}H NMR spectroscopy. After 65 min at 25 °C, the Pt—Tol*H* signals for the $(N^f{-}N^f)Pt(Tol)(H_2O)^+$ complexes had decreased by ca. 16% relative to the original intensity due to deuterium incorporation from toluene-d_8. Albeit an analysis of the rate of toluene activation at the mixture of $(N^f{-}N^f)Pt(Tol)(H_2O)^+$ complexes is complicated by H/D scrambling processes and possible kinetic isotope effects, this experiment indicates that the reaction is considerably slower than the activation of toluene at **1**.

X-ray Crystallographic Structure Determination of 3a. Crystals were obtained by slow evaporation of a dichloromethane solution of **3a**. X-ray data were collected on a Siemens SMART CCD diffractometer[31] using graphite-monochromated Mo Kα radiation. Data collection method: ω-scan, range 0.6°, crystal-to detector-distance 5 cm; further information is given in Table 2. Data reduction and cell determination were carried out with the SAINT and XPREP programs.[31] Absorption corrections were applied by the use of the SADABS program.[32]

The structures were determined and refined using the SHELXTL program package.[33] The non-hydrogen atoms were refined with anisotropic thermal parameters; hydrogen positions were calculated from geometrical criteria with isotropic thermal parameters. Final figures of merit are included in Table 2. The structure was refined in the space group *Pnma* (the use of $Pna2_1$ did not alter the geometrical features).

Acknowledgment. We gratefully acknowledge generous support from the Norwegian Research Council, NFR (stipend to L.J.).

Supporting Information Available: X-ray crystallographic file, listings of crystal data, X-ray experimental details, atomic coordinates, thermal parameters, and bond distances and angles for *syn*-**3b** (CIF). This material is available free of charge via the Internet at http://pubs.acs.org.

JA010277E

(31) SMART and SAINT Area-detector Control and Integration Software; Siemens Analytical X-ray Instruments Inc., Madison, WI, 1996.

(32) Sheldrick, G. M. Private communication, 1996.

(33) Sheldrick, G. M. SHELXTL, Version 5; Siemens Analytical X-ray Instruments Inc., Madison, WI, 1998.